JOURNAL OF GEOPHYSICAL RESEARCH, VOL. 101, NO. D3, PAGES 7033–7047, MARCH 20, 1996

New theoretical framework for studies of vapor growth and sublimation of small ice crystals in the atmosphere

J. T. Nelson
National Center for Atmospheric Research, Boulder, Colorado

M. B. Baker
Geophysics Program, University of Washington, Seattle

Abstract. We present a new microscopic model of growth and sublimation (g/s) of ice crystals in the atmosphere. This model is based on the assumption that the flux of vapor to the crystal surface is uniform over each flat crystal face. It thus differs fundamentally from the standard "capacitance" model for crystal growth, in which the mixing ratio is assumed uniform at the surface. In the new model the surface influence on growth is calculated self-consistently in terms of local environmental conditions, again differing sharply from the standard models in which this influence is either ignored or assigned a uniform, externally prescribed value. The new model leads to predictions of the evolution of ice crystal shape as well as mass. We find that predicted g/s rates are generally smaller than those predicted by the earlier models. The general trends both in g/s rates and in crystal hollowing predicted by the model are consistent with field and laboratory observations. The values of certain surface parameters needed for application of our model must be found from experiment. We review and compare the relevant laboratory experiments on ice crystal g/s rates and show their lack of mutual consistency. Therefore the surface parameters inferred from these experiments are necessarily uncertain. We show that the surface parameter values can be inferred from observations of crystal hollowing, since our model allows the prediction of environmental conditions at which hollowing should occur.

1. Introduction

1.1. Calculating Growth and Sublimation Rates

1.1.1. Need for a new framework. Vapor grown atmospheric ice crystals are found in a wide range of thermodynamic regimes. In mixed phase clouds, strong updrafts or downdrafts the crystals experience conditions very far from equilibrium. Their growth/sublimation (hereafter g/s) rates are rapid and largely determined by the rates of diffusion of heat and moisture to and from the crystal. Under these conditions the usual "capacitance" model yields quantitatively accurate results for the rate of mass uptake, although it does not contain any information on crystal shape evolution.

On the other hand, in and near ice clouds at weak updrafts/downdrafts in the upper troposphere and stratosphere the environmental conditions near crystals are closer to equilibrium, and because vapor pressures are low, the crystals are quite small. Recent observations [*Arnott et al.*,1994; *Ström and Heintzenberg*, 1994] show that in and near cirrus the numbers of crystals whose linear dimensions do not exceed around 70-100 μm may be far larger than previously suspected. The g/s rates of these small ice particles may be determined largely by processes occurring on the crystal surfaces, rather than in the gaseous crystal environment. The capacitance model does not incorporate these processes and may significantly overestimate g/s rates for these crystals. In this paper we develop a theoretical framework for the study of ice crystal g/s rates which is applicable throughout the entire range of atmospherically realistic conditions. Our results show that in and near fully glaciated clouds the capacitance model can significantly overestimate g/s rates, and we show the dependence of the error as a function of crystal shape and size.

In all atmospheric conditions the ice crystal shape is determined by processes which occur on the crystal surfaces. The shapes, as well as sizes, are important determinates of the radiative properties of ice clouds [*Kinne and Liou*, 1989]. Our model framework allows prediction of the crystal aspect ratios as functions of time and environmental conditions during steady state g/s given certain assumptions about the surface growth mechanism, and it also predicts the environmental conditions under which steady state g/s ceases and crystal hollowing begins. We present these predictions and laboratory evidence supporting them.

The organization of this paper is as follows. The rest of the introduction contains a discussion of the problems with the existing treatments of ice crystal growth. In section 2 we review the formalism for computing the g/s rate of a spherical crystal, taking advantage of the simplicity of that system to present the basis for the calculations to follow. The g/s rates we derive are functions of the surface impedance, and we discuss several models for this impedance in section 3. In section 4 we develop a model for g/s rates of nonspherical flat-faced crystals, present the resulting g/s rates for a range of crystal parameters, and compare these calculations to those from the capacitance model. In section 5 the new model is applied to the determination of ice crys-

Paper number 95JD03162.
0148-0227/96/95JD-03162$5.00

tal shape evolution. Section 6 contains a discussion of the new model and its predictions for both g/s rates and crystal hollowing in the light of atmospheric and laboratory observations. Further applications of this model to ice crystal g/s in the real atmosphere are discussed in section 7. Appendix A contains a list of symbols used in the equations to follow.

1.1.2. Basis for the new model. There have been 2 different approaches to the problem of calculating ice crystal growth rates. The most common approach is based on 2 assumptions: (1) the water vapor mixing ratio at the surface is uniform and in equilibrium with the ice,

$$q_s = q_{eq}(T_s)\ [(\mathrm{kg\ H_2O})/(\mathrm{kg\ air})], \qquad (1)$$

and (2) the crystal shape is approximated as an ellipsoid of revolution.

The first assumption makes the vapor growth problem analogous to the problem of computation of the electrostatic potential surrounding a capacitor with the shape of the crystal, so this model for g/s is called the "capacitance" model. Equation (1) cannot hold exactly for a growing or sublimating crystal since the mass uptake of the crystal depends only on the vapor mixing ratio at the surface, and the surface vapor mixing ratio is exactly in equilibrium with the surface only when the crystal is in equilibrium. A more basic difficulty is the fact that the vapor flux to the surface calculated from equation (1) would not be uniform over a crystal face and therefore it could not produce the observed faceted ice crystal growth shapes. Moreover, ice crystals are not ellipsoidal in shape. Observations [*Heymsfield and Platt*, 1987; *Sassen et al.*,1989b; *Ramaswamy and Detwiler*, 1986.; *Arnott et al.*,1994] show that most ice crystals in cirrus are hollow or solid hexagonal columns or thick plates of aspect ratio $\Gamma \equiv c/a$ between 0.1 and 10, where 2c is the crystal length along the c-axis and 2a the length along the minor a axis.

A newer approach to the study of g/s rates [*Kuroda*, 1984; *Mackenzie and Haynes*, 1992] uses a physically realistic boundary condition at the surface, but approximates the ice crystal as a sphere. A new model is needed that is based on a physically realistic boundary condition and incorporates realistic crystal shapes.

Surface transport processes control the rate of deposition and sublimation of molecules at the ice/vapor interface. We define a function, α, that varies over the crystal surface and is equal to the fraction of molecules incident on the surface that become incorporated into the crystal at each point. Since α is always less than 1, growth is impeded by the processes that determine α. We show below that the surface impedance to the flux of vapor to a crystal is 1/α.

We assume the surface transport processes do not redistribute molecules across dimensions of order of the face width. This is consistent with the experiments of *Mason et al.* [1963] if the crystal faces are larger than ~10 μm across. Then the correct boundary condition for uniform growth of crystals is that the vapor flux to each crystal face must be uniform over that face; that is,

$$D_g \frac{\partial q}{\partial z}\bigg|_{\mathrm{face}} \equiv F_v\,[\mathrm{kg\ H_2O/kg\ air\ m^2 s}] = \mathrm{uniform}, \qquad (2)$$

where D_g [m^2/s] is the vapor diffusivity and z is the coordinate normal to the crystal face. (The electrostatic analog is that of a uniform electric field, instead of a uniform potential at the crystal surface.)

Previous authors [e.g., *Mason*, 1993] have argued that both equation (1) and the uniform flux condition (equation (2)) can hold. In their model, uniform flux is maintained through a surface transport process from a region of higher vapor diffusive flux to a region of lower diffusive flux. However, it is unlikely that such a process could ever completely compensate for a nonuniformity in vapor diffusive flux (even if the molecules could migrate across large distances). Moreover, surface transport should not produce a flux of molecules away from growth sites. (Those sites at which the molecules are most strongly bound.) In this paper we use equation (2) as the surface boundary condition to derive analytic expressions for the g/s rates of stationary, finite circular cylinders.

2. G/S Rates of Spherical Crystals

In the absence of airflow the mixing ratio q and temperature T adjacent to the crystal satisfy the steady state Laplace's equations;

$$\nabla^2 q = 0, \qquad (3)$$

$$\nabla^2 T = 0. \qquad (4)$$

At large distances from the crystal the mixing ratio and temperature approach their ambient values, q_∞ and T_∞, respectively. The temperature approaches T_s near the crystal surface. The surface vapor boundary condition is developed below.

The boundary condition on q at the surface determines the mixing ratio at the crystal surface, q_s, and hence the vapor flux to the crystal. This boundary condition is therefore a very important element of a crystal growth model and will be the focal point for discussion in later sections. The vapor flux to the surface, determined from the solution to equation (3), is

$$F_v \equiv D_g \frac{dq}{dr}\bigg|_a = D_g \frac{q_\infty - q_s}{a}, \qquad (5)$$

where a is the crystal radius. We require (equation (2)) that the flux be uniform over the surface. (For the spherical geometry this is consistent with uniform q_s.) For small departures from equilibrium, we can write

$$F_v = \alpha \frac{\bar{v}}{4}(q_s - q_{eq}(T_s)) \equiv \alpha \frac{\bar{v}}{4} q_\infty \sigma_s, \qquad (6)$$

where $\bar{v} = \sqrt{(8kT)/(\pi m)}$ is the mean thermal velocity of a water vapor molecule of mass m. Equation (6) defines α, also known as the condensation (deposition) coefficient; $0 \le \alpha \le 1$. The condensation coefficient (α) depends on the surface supersaturation (σ_s). In section 3 we introduce several models of this dependence, based on current theoretical ideas on the nature of the crystal surface. Then we obtain self-consistent values of $\alpha(\sigma_s)$ and the growth rate in terms of the environmental conditions and surface properties.

The flux of heat to the surface is due to the exchange of energy from air molecules colliding with the surface. Since an air molecule is heavier than a water molecule, the energy transfer incident from an air molecule to the surface is expected to be very efficient [*Goodman*, 1980]. Therefore the air molecules should acquire a velocity distribution characteristic of the surface temperature. The thermal accommodation coefficient, which is a measure of the efficiency of this energy transfer, should be close to 1 and the resulting heat flux is very nearly given by

$$F_h = \kappa_g \frac{dT}{dr}\bigg|_{r=a} \quad [\mathrm{W/m^2}] \tag{7}$$

where κ_g is the thermal conductivity in the environment. The solution of equation (4) subject to the appropriate boundary conditions is analogous to that (equation (5)) for the vapor mixing ratio.

In general, the crystal absorbs and emits radiation from its environment. However, our calculations suggest that for realistic atmospheric temperature profiles the effect of radiative exchange on crystal g/s rates is generally small unless the crystal dimensions are greater than approximately 50 μm and the humidity is within approximately 5% of equilibrium. This situation may not be uncommon, but for simplicity we ignore the radiative effects in this paper. Their addition represents a straightforward modification to the results we will present here and simply translates the effective supersaturation experienced by a particle, raising it during radiative cooling and lowering it during heating.

We assume that the conductive and latent heat fluxes balance at the crystal surface

$$F_h + \frac{l\rho_{air}}{m} F_v = 0, \tag{8}$$

where l (J/molecule) is the latent heat of sublimation/molecule and ρ_{air} [kg m^{-3}] is the density of moist air.

For $T_s - T_\infty$ sufficiently small, the Clausius-Clapeyron equation can be linearized and from eqs. (5), (6), and (8) we can solve for F_v. We define the nondimensional total volume impedance as the sum of the vapor and thermal impedances

$$a'_{tot} \equiv \frac{\bar{v}a}{4D_g} + \frac{a\bar{v}kq_\infty \rho_{air}}{4\kappa_g m} l'(l'-1) \equiv a'_v + a'_{th}, \tag{9}$$

where $l' \equiv l/kT_\infty$. The resulting vapor flux to the crystal is

$$F_v = \frac{\frac{\bar{v}}{4} q_\infty \sigma_\infty}{1/\alpha + a'_{tot}}, \tag{10}$$

where the far-field supersaturation (σ_∞) is given by

$$\sigma_\infty \equiv \frac{q_\infty - q_{eq}(T_\infty)}{q_\infty}. \tag{11}$$

The numerator represents the maximum, so-called Wilson-Frenkel flux [see, for example, *van der Eerden*, 1993], while the two terms in the denominator represent impedances to growth due to surface transport ($1/\alpha$) and volume transport (a'_{tot}). The relationship between vapor flux and σ_∞ in equation (10) is analogous to that between current and voltage in an electrical circuit; the terms in the denominator of eq (10) play the roles of impedances to the "current" (vapor flux) driven by the "voltage" (environmental humidity). Equation (10) is identical to the result obtained by other authors [*Fukuta and Walter*, 1970; *Kuroda*, 1984; *MacKenzie and Haynes*, 1992].

From eqs. (6) and (10)

$$\sigma_s = \frac{\sigma_\infty}{1 + a'_{tot}\alpha}, \tag{12}$$

so that for $a'_{tot} \cdot \alpha \gg 1$ (vapor impedance>>surface impedance) the surface supersaturation goes to zero; that is, the mixing ratio adjacent to the surface approaches its equilibrium value. Conversely, when $a'_{tot}\alpha \ll 1$, $\sigma_s \approx \sigma_\infty$.

The growth rate is found from equation (10):

$$\frac{da}{dt} = \frac{\rho_{air}}{\rho_{ice}} F_v, \tag{13}$$

where ρ_{ice} [kg m^{-3}] is the density of ice.

The vapor impedance (a'_v) depends on the mean free path for water vapor molecules ($\approx D_g/\bar{v}$) and the crystal radius. In the atmosphere the mean free path increases with altitude due to the decrease in pressure. More importantly, the mean observed crystal sizes decrease with altitude at cold temperatures because of lower growth rates. At high altitudes a 20 μm diameter ice crystal has a vapor impedance of approximately 20.

The thermal impedance (a'_{th}) is also proportional to the crystal radius. The ratio of the thermal impedance to the vapor impedance is roughly 1.3 at 0°C, but drops rapidly to <0.1 for $T \le -40$°C. Its rapid decrease with temperature is due to the rapid decrease of q_∞ ($\approx q_{eq}(T_\infty)$) with T_∞. Therefore in most ice phase clouds the thermal impedance can be neglected. We now examine the surface impedance.

3. Surface Impedance

We can now compute the growth rate of a spherical crystal via equation (10) if we have a model for $\alpha(\sigma_s)$. We adopt a picture of the ice surface based on ideas that are quite generally applicable to crystals in gaseous environments. Each crystal face is assumed to be a macroscopically flat plane of dimensions much larger than the mean free path in the gaseous environment (water vapor in air). We assume that each face consists of regions relatively devoid of positions for permanent attachment, called terraces, and regions relatively rich in them, called ledges. Molecules arriving from the vapor phase strike the terrace, stick, and a fraction of them (α) then migrate to a ledge. The remaining molecules desorb before reaching a ledge and do not grow into the crystal. Transport along the terrace may take place via individual molecular hopping on the terrace as in surface diffusion, or it may be a more complicated cooperative phenomenon.

Little is known experimentally about the detailed structure of the ice/vapor interface: until recently most observations lacked the necessary resolution to reveal features at the necessary scales. In a study of crystals grown on glass, *Sei and Gonda* [1989] found evidence supporting the idea [*Burton et al.*, [1951]; hereafter referred to as BCF] that the surface consists of many, locally equidistant ledges formed continually via line dislocations which intersect the surface. On the other hand, *McKnight and Hallett* [1978], and *Mizuno* [1978] found that crystals growing free of attaching surfaces at temperatures near -15C and -3C grew with dislocation free surfaces, suggesting that under these conditions the ledges are the edges of 2-D nuclei, as suggested also by *Frank* [1982]. Thus it appears that ice crystal growth free of attaching surfaces (as in the atmosphere) usually occurs via 2-D nucleation while sublimation occurs via ledges receding from the crystal edges [*Shaw and Mason*, 1955].

The surface impedance to g/s can be calculated for each model of ledge generation and surface transport. We propose here a 2 parameter equation to approximate $\alpha(\sigma_s)$ for a variety of ledge generation mechanisms and surface processes:

$$\alpha(\sigma_s) = \left(\frac{\sigma_s}{\sigma_1}\right)^n \tanh\left[\left(\frac{\sigma_1}{\sigma_s}\right)^n\right], \qquad (14)$$

where σ_1 and n are properties of each crystal face and depend on temperature. Qualitatively, the basic features of the $\alpha(\sigma_s)$ relationship are common to 2-D nucleation and to all other ledge generation mechanisms, as shown in Figure1, where we plot equation (14) for $n = 1$ (the form consistent with the BCF mechanism), and schematic curves for stacking fault-induced nucleation [*Ming et al.*,1988] and ledge nucleation. In all cases, $\alpha \to 0$ as $\sigma_s \to 0$ and $\alpha \to 1$ as $\sigma_s \to \infty$; the surface impedance becomes increasingly important as the ambient supersaturation is reduced. Unfortunately, this low supersaturation regime has not been well explored experimentally.

Given the similar qualitative behavior predicted for all these mechanisms and the apparent experimental evidence that nucleation predominates as a general rule in the atmosphere, at least in growth, we will use equation (14) with $n > 1$ to represent the relation between α and σ_s as appropriate in the rest of this paper. However, as an algebraically simple illustration of our procedure for computing the g/s rates, we assume n=1 in equation (14) and use equation (12) (which relates α, σ_s, and σ_∞) to calculate α as a function of the environmental conditions and the crystal size. Assuming that $\tanh(\sigma_1/\sigma_s) \sim 1$, it follows that

$$\alpha \cdot a'_{tot} = \sqrt{\frac{1}{4} + \frac{\sigma_\infty}{\sigma_1} a'_{tot}} - \frac{1}{2}. \qquad (15)$$

The flux of vapor to the crystal surface (and thus the crystal growth rate) can be found by substituting equation (15) into equation (10). The left-hand side of equation (15) is the ratio of the volume impedances to the surface impedance. Vapor/heat diffusion is growth rate controlling when $\alpha \cdot a'_{tot}$ is large, while from equation (15), we see that at low ambient supersaturations and small crystal sizes this ratio is small, and surface impedance is the limiting factor in crystal growth. This behavior would also have been obtained if we had used a larger value of n in this derivation.

The results of this section are shown schematically in Figure 2. The volume impedances are g/s rate limiting for high temperatures and large crystals (i.e., in mixed phase clouds); in strong updrafts at colder temperatures the vapor diffusion impedance is more important than the thermal impedance, and in typical upper tropospheric and stratospheric conditions the surface impedance becomes important. The qualitative features of these results are independent of the details of the surface processes and depend only on the general behavior of $\alpha(\sigma_s)$ shown in Figure 1.

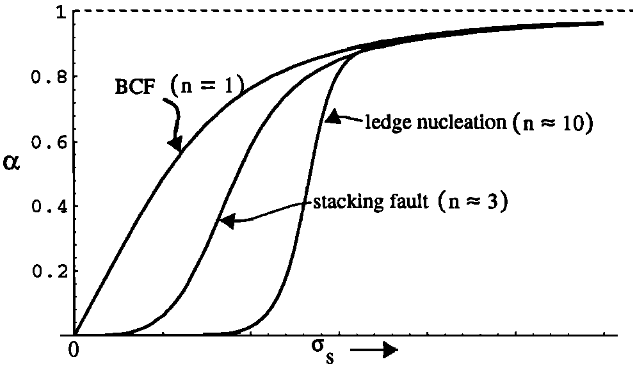

Figure 1. Schematic curves of the condensation coefficient as a function of surface supersaturation for several ledge formation models.

4. Nonspherical Crystals

In this section we derive the g/s rates of crystals of the simplest shapes with flat faces starting with the infinitely thin disk that receives flux only over its top and bottom faces. In section 4.2 we use the formalism derived for this case to discuss the somewhat more realistic case of circular cylindrical crystals of finite height. Circular cylinders have 2 types of face, each with its own intrinsic surface processes. The evolution of crystal shape in then discussed in section 5.

4.1. Vapor Diffusion to a Thin Disk

Using the notation of the previous chapter, we solve Laplace's equation for the mixing ratio outside the disk subject to the boundary condition that the flux is uniform on the top and on the bottom of the disk. It is convenient to define nondimensional variables which we denote by primes,

$$z' \equiv \frac{z}{a}, r' \equiv \frac{r}{a}, \Delta q' \equiv \frac{q - q_\infty}{q_\infty}, \qquad (16)$$

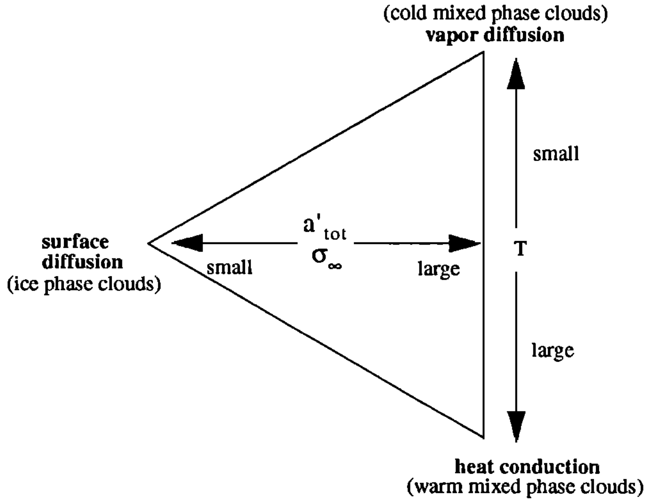

Figure 2. The growth rate limiting processes for ice crystals in different regions of the atmosphere.

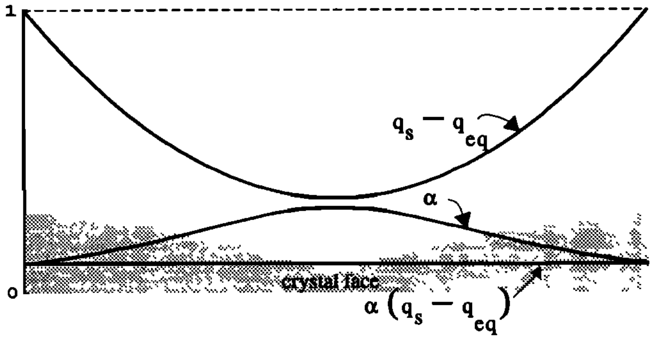

Figure 3. Variation of mixing ratio and α across a crystal face showing ledge positions calculated using the BCF model of surface diffusion.

where r is now the cylindrical radial coordinate and a is the disk radius. The nondimensionalized, boundary condition becomes

$$F'_v \equiv \frac{\partial}{\partial z'}\Delta q' = \alpha a' \sigma_s \quad (r' < 1, z' \rightarrow 0)\,. \tag{17}$$

With the above boundary condition the nondimensionalized solution of Laplace's equation is

$$\Delta q'(r', z') = -F'_v h(r', z')\,, \tag{18}$$

where h is defined in *Seeger* [1953]. It represents the solution for unit flux.

The nonspherical geometry introduces a fundamentally new issue into the problem of crystal growth. That is; all points on the surface are no longer equivalent, so that since the normal gradient of q is uniform, q_s will not generally be uniform. We must now add a physical assumption about the variations of α and σ_s on the surface to be able to proceed. Our assumption is that α is determined everywhere by its value at the ledge source positions. (These can be at dislocations, at other kinds of defects, or at crystal edges, and the ledges may be regularly spaced steps or the edges of 2-D nuclei.) It is here that α is controlled by the local mixing ratio (via equation (14)). As ledges collect surface admolecules and move away from their source, the local supersaturation to which they are subject will change. In regions of lower (higher) supersaturation the ledge spacing will be smaller (larger), and therefore 1/α, which is a measure of the difficulty of surface transport to ledges, will be smaller (larger); that is, α will be larger (smaller). For uniform growth the product $\alpha \cdot \sigma_s$ is uniform, as was assumed by, e.g., *Kobayashi and Kuroda* [1987]. Our procedure is to relate α to σ_s via equation (14) at the ledge source position, and thus to find the flux there. We then require that α and σ_s vary with position on the surface in such a way as to keep their product (i.e., the vapor flux) uniform everywhere. (See Figure 3.) Thus

$$F'_v = \alpha(r') a' \sigma_s(r') = \alpha(r') a' (\Delta q'_s(r') + \sigma_\infty)\,. \tag{19}$$

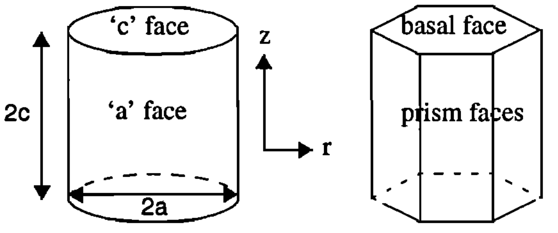

Figure 4. Variables and coordinates in the cylinder diffusion problem.

We insert equation (18) into equation (19) to solve for F'_v, but the solution will depend on the crystal temperature. Solving the heat conduction equation in order to remove the dependence on crystal temperature is exactly analogous to the problem encountered for the sphere and will not be repeated here. The solution is

$$F_v = \frac{\frac{\bar{v}}{4} q_\infty \sigma_\infty}{1/\alpha(r') + a'_{tot} h(r', 0)}\,. \tag{20}$$

Note the resemblance to the spherical crystal case, equation (10).

In contrast to the spherical crystal case, F_v does not approach the capacitance model limit when $\alpha a'_{tot} \rightarrow \infty$, although $\sigma_s \rightarrow 0$ in this limit. This is because equation (20) is derived for the case that the flux remains uniform across the disk. Physically, the zero surface impedance, uniform growth limit cannot be attained; surface kinetic processes are required to keep the flux uniform on each face.

Using the notation and procedure introduced for the limiting case of an infinitely thin disk, we next derive the g/s rate for a finite cylinder.

4.2. Growth Rate of a Finite Cylinder

For most atmospheric conditions a solid ice crystal is bounded by 2 types of faces: basal and prism. This shape is similar to that of a circular cylinder. We assume the crystals are circular cylinders in this development for analytic simplicity, although our general discussion also applies to hexagonal columns. (See Figure 4.)

The present treatment now closely follows that in the previous section. We assume now that the flux is determined by its value at the ledge sources. We must therefore know where the ledge sources are on both the 'a' face and the 'c' face. At low supersaturations the ledges can only originate at bulk dislocations or faults, and these could be anywhere on a face (if present at all). When the supersaturation (σ_∞) becomes large enough to nucleate ledges on the surface, the expected positions for ledge sources are the regions of highest supersaturation. For simplicity we will assume that the region of ledge nucleation is at the edges (Figure 5), although this probably is not the case for crystals with very anisotropic growth rates [*Nelson*, 1994; also see Figure 9]. Knowledge of the ledge source positions allows us to find the g/s rates of each face and the total rate of mass uptake if the surface impedance $(1/\alpha)$ is known on each face. We summarize the calculations below for the case that the ledge sources are at the crystal edges and our results are given in equations (25) and (27). The reader who wishes to skip mathematical details can proceed directly to section 4.3.

We define

$$\Gamma \equiv \frac{c}{a}, \quad c'_v \equiv a'_v \Gamma, \tag{21}$$

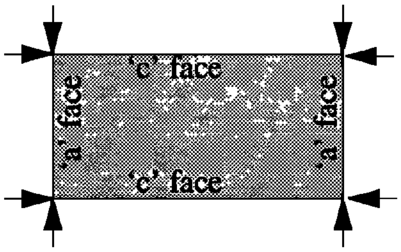

Figure 5. Cross section of an ice crystal showing the assumed positions of the ledge sources.

and the fluxes to the 'c' ('a') faces, F'^{c}_{v}, and F'^{a}_{v},

$$F'^{c}_{v} \equiv \frac{\partial}{\partial z'}\Delta q'\big|_{(r',1)},\quad F'^{a}_{v} \equiv \frac{\partial}{\partial r'}\Delta q'\big|_{(1,z')}. \qquad (22)$$

The technique for solving $\nabla^2 q' = 0$ with uniform fluxes on both faces is described in *Nelson* [1994] (Appendix) and is summarized in Appendix B. The general solution for the mixing ratio can be written

$$\Delta q'(r', z', \Gamma) = -F'^{c}_{v} h^{c}(r', z', \Gamma) - F'^{a}_{v} h^{a}(r', z', \Gamma). \qquad (23)$$

Equation (23) is the analog of equation (18), and $h^{a,c}$ are the analogs of h for the thin disk case. Note that $-h^c$ is the mixing ratio when $F'^{c}_{v} = 1$, $F'^{a}_{v} = 0$, while $-h^a$ is that for $F'^{a}_{v} = 1$, $F'^{c}_{v} = 0$. Equation (23) shows that $\Delta q'$ is determined by the two fluxes $F'^{(c,a)}_{v}$. This same relation holds for hexagonal prisms with different h functions. Numerical values of $h^{c,a}$ for circular cylinders are given in Appendix B.

Next, in analogy with equation (19) we have

$$F'^{c}_{v} = \alpha^c c'_v \sigma_s((c)) = \alpha^c c'_v (\Delta q'\big|_{(c)} + \sigma_\infty), \qquad (24)$$

where we label the coordinates (r', z') of the ledge sources on the 'c' faces *(c)*. An analogous equation holds for the 'a' face. Using equations (23) and (24), we can solve for the fluxes and express them as functions of a'_v, c'_v, Γ, α^a, α^c, σ_∞, and the positions of the ledge sources in a manner analogous to that presented in the thin disk section.

Following steps similar to those in our spherical crystal calculation and assuming that heat conduction into the crystal can be neglected, it is straightforward to show that

$$F^{c}_{v} = \frac{\alpha^c \cdot q_\infty \frac{\bar{v}}{4}\sigma_\infty}{1 + \alpha^a a'_{tot} h^a(\Gamma) + \alpha^c c'_{tot} h^c(\Gamma)} = \frac{\rho_{ice}}{\rho_{air}}\frac{dc}{dt}, \qquad (25)$$

where $c'_{tot} \equiv c'_v + c'_{th}$ with $c'_{th} \equiv c/a \cdot a'_{th}$. An analogous formula holds for the 'a' face, with α^a instead of α^c in the numerator. The second and third term in the denominator of equation (25) is the total volume impedance divided by the surface impedance for the 'c' faces. (In ice clouds c'_{th}, a'_{th} is usually much smaller than c'_v, a'_v so that the thermal impedance term can be neglected in this case.) Equation (25) together with a model of $\alpha^a(\sigma_s)$ and $\alpha^c(\sigma_s)$ allow us to calculate the growth rate of each face. These equations constitute the new model for vapor growth and sublimation of a cylindrical crystal.

It is useful to point out the similarities in the expressions for the vapor flux to various shaped crystals. For this comparison we divide the fluxes by the factor $q_\infty \bar{v}/4\sigma_\infty$ and present the normalized fluxes in Table 1 for a stationary crystal. The table shows that in all cases the net vapor flux is diminished by a factor of the form $\alpha/(1 + \alpha a'h)$, where the $\alpha a'h$ terms in each denominator is the ratio of the surface to the volume impedance. The sphere and thin disk are special cases for a crystal with only 1 "type" of face, while the finite cylinder is a special case of a crystal with 2 "types" of faces. Equation (25) can thus be generalized to the case of an arbitrary number of independent faces.

To obtain the growth rate, $\alpha^{c,a}$ must be known in terms of the environmental conditions. First we must find the supersaturation at the crystal surface. For edge ledge sources, setting equation (24) equal to equation (25)

$$\sigma_s((a)) = \frac{\sigma_\infty}{1 + \alpha^a a'_{tot} h^a(\Gamma) + \alpha^c c'_{tot} h^c(\Gamma)} = \sigma_s((c)). \qquad (26)$$

As was the case for a spherical crystal (equation (15)), the solution to equation (26) when substituted in the expressions for $\alpha^{c,a}(\sigma_s)$ gives the surface impedances as a function of the ambient conditions.

The fluxes to the crystal in the uniform flux model are given by equation (25), using the solutions to equation (26) for α^c and α^a. When $\Gamma = \alpha^c/\alpha^a$ (the condition for steady state growth, as we show in section 5.1, the resulting mass uptake is

$$\frac{dM}{dt} = \frac{\rho_{air}\sigma_\infty q_\infty \frac{\bar{v}}{4}(2\pi ac)\cdot 3\alpha^a}{1 + \alpha^a a'_{tot}\{h^a(\Gamma) + \Gamma^2 h^c(\Gamma)\}}, \qquad (27)$$

where M is the crystal mass.

4.3. Predicted Growth Rates

We now compare the predictions of our model to those of the capacitance model to delineate the parameter regimes in which the two give the same results and those in which

Table 1. Normalized Vapor Flux for Various Crystal Shapes

Sphere	Thin Disk	Finite Cylinder
$\dfrac{\alpha}{1 + \alpha a'_{tot}}$	$\dfrac{\alpha}{1 + \alpha a'_{tot} h}$	$\dfrac{\alpha^{(a,c)}}{1 + \alpha^a a'_{tot} h^a(\Gamma) + \alpha^c c'_{tot} h^c(\Gamma)}$
Equation (10)	Equation (20)	Equation (25)

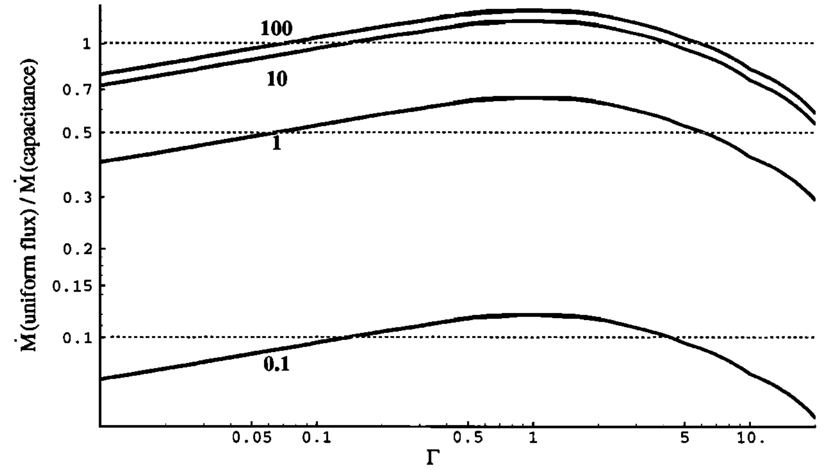

Figure 6. Comparison of the total steady state mass uptake rate for the uniform flux finite cylinder model (equation (27)) to that predicted by the ellipsoidal capacitance model (equation (28)). The numbers give the ratio of the vapor impedance to the surface impedance.

their results are different. The surface impedance is considered negligible for all supersaturations in the capacitance model, whereas in our model the minimum possible value of $1/\alpha$ is 1.

We first compare the mass uptake rate predicted from equation (27) for a finite cylinder with that predicted from the capacitance model for an ellipsoid of the same aspect ratio. Since thermal impedance is usually neglected in the capacitance model, we neglect it in our model for this comparison. The rate of mass uptake of an ice crystal in the capacitance model is [see, e.g., *Wallace and Hobbs*, 1977]

$$\left.\frac{dM}{dt}\right|_{cap} = \rho_{air}\sigma_{\infty}q_{\infty}\frac{\bar{v}}{4}\,(4\pi ac\mathrm{Cap}/ca'_{v})\,, \qquad (28)$$

which is to be compared with equation (27). Cap is the capacitance (in esu) for a conductor with the same shape as the crystal. The capacitance of an ellipsoid can be computed exactly as a function of the aspect ratio Γ [*Morse and Feshback*, 1953.]

The results of this comparison are shown in Figure 6. As was the case for spherical crystals (see equation (12)), when the surface impedance is much smaller than the volume impedance, the mixing ratio adjacent to the surface is very close to equilibrium (although it remains nonuniform), so the mass uptake in the finite cylinder and ellipsoid capacitance models are in close agreement in this limit. Since a finite cylinder has a larger surface area than an ellipsoid for a given value of c and a, the finite cylinder uniform flux mass uptake can exceed that from the ellipsoidal capacitance model for small surface impedances. However, the capacitance model significantly overestimates the mass uptake when the surface impedance is significantly larger than the vapor impedance. Note that $\alpha^{(a,c)}$ rises with σ_s and thus with σ_∞. Hence for high σ_∞ or large crystals the ratio of volume to surface impedance is large and the capacitance and the finite cylinder model lead to very similar g/s predictions. Therefore the capacitance model for mass uptake is probably accurate in mixed-phase clouds (except near 0°C), where crystal size and supersaturation are both large, but it is not likely to be applicable in ice phase clouds. In and near ice phase clouds the capacitance model probably overestimates the g/s rates. This is illustrated in Figure 7 which shows how the linear growth rates predicted for $\Gamma = 1$ in the uniform flux model vary with condensation coefficient functions (equation (14)). Note that for large n the flux is significantly reduced even for $\sigma_\infty > \sigma_1$.

4.4. Predicted Sublimation Rates

Ledge source mechanisms for growth can also operate as ledge sources for sublimation. (Instead of nucleating islands, holes are nucleated.) In addition, the crystal edges can serve as ledge sources for sublimation. Physically, we expect that the generation of ledges from the edge is similar to a nucleation process although the critical undersaturation might be very low. Impurities in or on the surface could increase this critical undersaturation [*Surek*, 1972; *Nelson*, 1994]. If the undersaturation is significantly larger than the critical value, then the edges of the crystal will round and

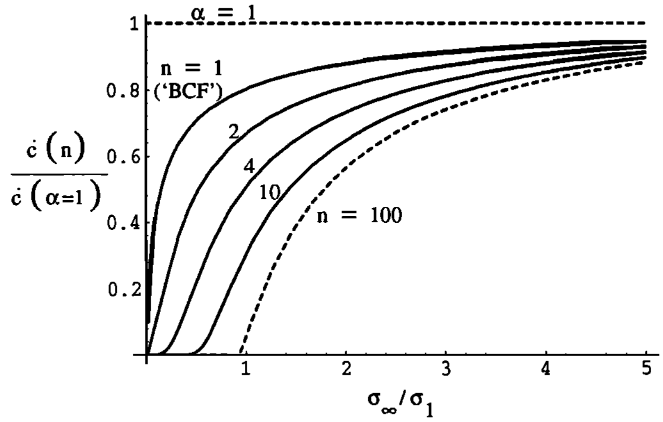

Figure 7. Growth rates in the uniform flux model with n and σ_1 defined in equation (14). The vapor impedance is set to 10, and $\alpha^c = \alpha^a$.

Table 2. Time in Seconds for a Columnar Crystal With σ_1^c=10%, σ_1^a=11%, n^c=10, n^a=10, and an Initial Size of c=60 μm, a=20 μm to Sublimate to One Half of Its Initial Size for Various Undersaturations

Undersaturation	5%	10%	20%	50%
Finite cylinder uniform flux	82000	2710	640	256
Ellipsoidal capacitance	1435	717	359	143

the uniform flux boundary condition no longer applies. When this is not the case, the sublimation process is simply the reverse of the growth process, and the technique given above applies. Shown in Table 2 are the ice crystal lifetimes in the ellipsoidal capacitance model and the finite cylinder uniform flux calculation. A large critical undersaturation can significantly increase the crystal lifetimes.

5. Crystal Shape

5.1. Crystal Habit in Uniform Growth

For ledge sources at the edge, equation (25) gives the ratio of the growth rate on the 'c' (basal) face to that on the 'a' (prism) face

$$\frac{dc}{da} = \frac{\alpha^c}{\alpha^a}. \qquad (29)$$

Physically, this is because the rate of ledge nucleation (and hence growth rate) is proportional to the excess number of molecules striking the surface (σ_s) times the probability of growing into the crystal (α), that is, $\alpha \cdot \sigma_s$ (equation (24)). For edge growth, σ_s at the ledge sources is the same for both faces, so that the ratio of the growth rates is simply the ratio of the condensation coefficients. This ratio is, in general, a function of temperature, crystal size, and the ambient supersaturation. In practice, $\alpha^{c,a}(\sigma_s)$ could be derived from experiment by fitting crystal g/s rates measured in a pure vapor of known supersaturation (where diffusive and thermal impedances would be negligible) to this model. These values could be inserted into the relation between σ_s and σ_∞ (equation (26)). The fluxes to each face would then be determined and the ratio in equation (29) could be deduced for a known set of ambient conditions.

If $\alpha^{c,a}(\sigma_s)$ were known, equation (29) could be integrated to obtain Γ as a function of c or a. One application of the results might be a comparison with the observations of *Auer and Veal* [1970] which were fit to the function

$$c = g \cdot a^\beta, \qquad (30)$$

where g and β are temperature dependent. However, it is not clear this comparison would be useful: equation (30) was fit to data which include a significant fraction of crystals with dimensions greater than 100 μm, sizes at which ventilation might affect the shape. It is also not known if all of the observed crystals of a given type grew at the same ambient supersaturation. *Chen and Lamb* [1994] have derived equation (30) from a "mass distribution hypothesis" which was not derived from a crystal growth model and differs from equation (29). In our model, crystal shape changes as a function of time for 3 reasons: (1) α^c/α^a depends on the surface supersaturation (Figure 1), which generally decreases with crystal size (equation (26)); (2) the initial crystal shape (Γ) is generally not equal to dc/da so that the shape will change until Γ = dc/da; and (3) a crystal eventually hollows (section 6.3 and Appendix C), thus changing the total flux to the hollowed faces. Examples of shape evolution produced by our model are shown in Figure 8.

If the vapor diffusivity is increased for a fixed σ_∞ (as in the experiments of *Gonda* [1980]) then σ_s increases (equation (12)), so $\alpha^c, \alpha^a \rightarrow 1$ and use of equation (29) leads to the prediction dc/da → 1. This is what Gonda observed.

5.2. Predicted Limits on Uniform Growth

In this section we show that the requirements of uniform growth (i.e., growth maintaining flat faces) constrain the ratio of surface impedance to volume impedances. This constraint is independent of the model used for the surface impedance. We present arguments suggesting that hollowing in crystals (also known as lacunary growth and hopper development), often observed in the atmosphere, occurs when these constraints are not met. The growth of hollow crystals is discussed in Appendix C.

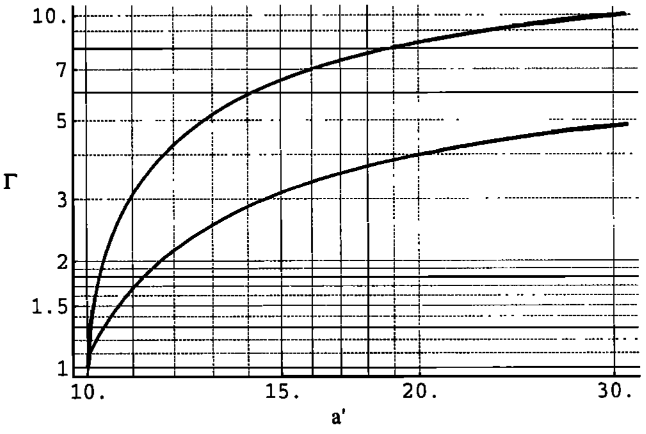

Figure 8. Changing crystal shapes during growth. Top curve: $\sigma_\infty, \sigma_1^c, \sigma_1^a$ = 0.5, 0.1, 1, and $n^{c,a}$ = 2, 4. Bottom curve: $\sigma_\infty, \sigma_1^c, \sigma_1^a$ = 0.5, 0.5, 1, and $n^{c,a}$ = 3, 4 (equation (14)).

To understand how hollowing occurs, one must first understand how uniform (flat faced) growth occurs. On the faster growing faces the surface supersaturation is greatest at the edge (see Figure 9). Therefore there are more vapor molecules striking the surface near the edge than near the face center, and if the surface ledges were equally spaced across the face then growth would be faster near the edge than near the center, resulting in a hollow crystal. This "destabilizing" effect is due to vapor diffusion and generally increases with the vapor impedance. However, the ledges are not evenly spaced across the face. The edge region, as a result of its having a larger supersaturation, is the preferred nucleation site. A ledge once nucleated there travels inward toward the face center. After traveling a certain distance (which is smaller for a larger supersaturation), a new ledge is nucleated. This process of producing equally spaced ledges near the edge results in a train of ledges traveling in toward the center of the face where the supersaturation is lower [*Frank*, 1982]. Since the ledge velocity is proportional to the local supersaturation, the ledges slow down as they approach the center. Like cars approaching a stop light, the ledges become closer together near the center and therefore collect a larger fraction of the incident vapor molecules. (See Figure 3.) The closing up of the ledges compensates for the decreasing local supersaturation and "stabilizes" uniform growth. The extent to which the surface ledges can stabilize uniform growth depends on the surface impedance. A large surface impedance means that the ledges are far apart at the edge and hence the ledges near the center need not be close together. In this case, growth is uniform across the face. From equation (24) this means that

$$\alpha \cdot \sigma_s = \text{uniform}. \qquad (31)$$

If the ambient supersaturation is increased (smaller surface impedance), the ledges near the center must become more efficient at collecting molecules. However, there are limits to this efficiency. In particular, the ledges cannot collect more molecules than strike the surface. Since α must always be less than 1, uniform growth becomes impossible when the condition equation (31) would require $\alpha(\text{center}) > 1$. In this case, the center must grow more slowly than the edge. Under these conditions the crystal is hollowing. An example is shown in Figure 10.

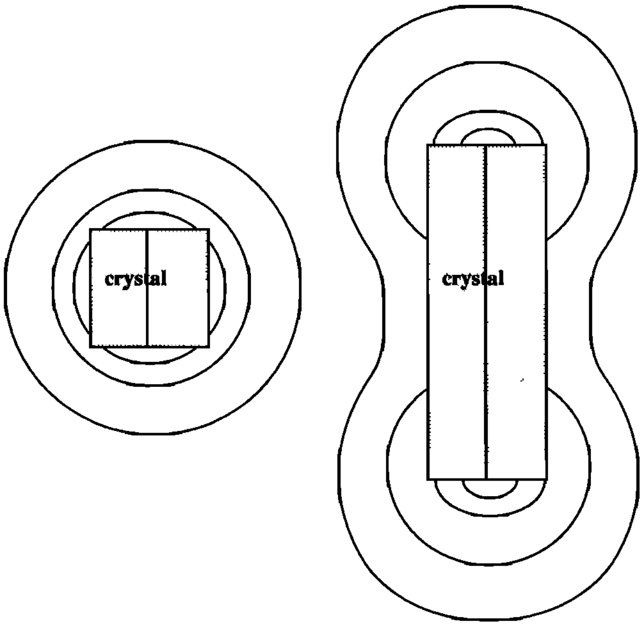

Figure 9. Schematic of the mixing ratio contours around an isometrically growing ice crystal (left) and an ice crystal growing fastest on its basal faces (right). Mixing ratio decreases as contours approach the surface.

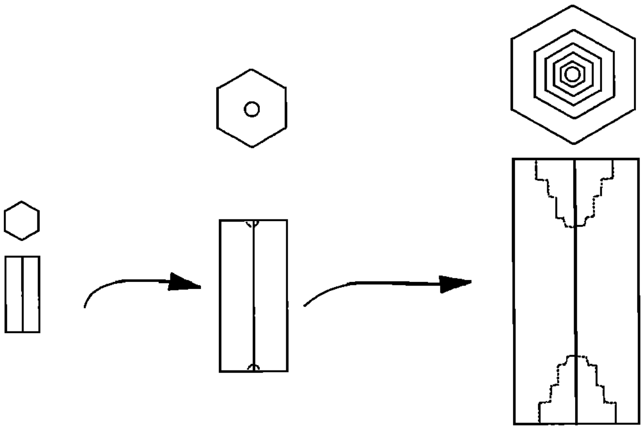

Figure 10. Schematic showing top and side view of a crystal hollowing on the 'c' faces as it grows (nonuniform growth).

At a given ambient supersaturation the difference in surface supersaturation between face center and edge increases with crystal size (and thus with vapor impedance), so that a larger ledge spacing at the edge (larger surface impedance) is needed for uniform growth on larger crystals. Therefore the uniform growth constraint sets a lower limit on the ratio of surface impedance to vapor impedance. From Figure 9 this relation is expected to depend on the relative rates of growth on the basal and prism faces. This is shown in Figures 11 and 12. For platelike growth the hollowing should occur on the 'a' faces (Figure 11), while for columnlike growth, hollowing is more likely on the 'c' faces (Figure 12).

The meaning of Figure 11 can be understood with the following example: Consider a crystal which begins growing at $\Gamma = 1$ (point i in the figure). As it grows, the vapor impedance (a'_v) generally increases faster than the surface impedance. If $da/dt > dc/dt$ $(\alpha^a > \alpha^c)$, its habit becomes platelike, so it follows a curve similar to the dashed curve shown in the figure. Near the point marked h, the surface impedance can no longer compensate for the difference in surface supersaturation between the edge and the center of the 'a' face and the crystal begins to hollow on that face. This process of nonuniform growth might continue, eventually producing sector plates or dendrites [*Frank*, 1982].

If instead the crystal grows into a columnar habit, it follows a curve like the dashed curve in Figure 12. The growth might continue in the nonuniform regime, eventually resulting in needle growth.

The dotted curves in Figures 11 and 12 indicate where hollowing would occur if $\Gamma = 1$ during growth $(dc/dt = da/dt)$. The maximum ratio of vapor to surface impedance for uniform growth is 4.0 on the 'c' face and 5.6

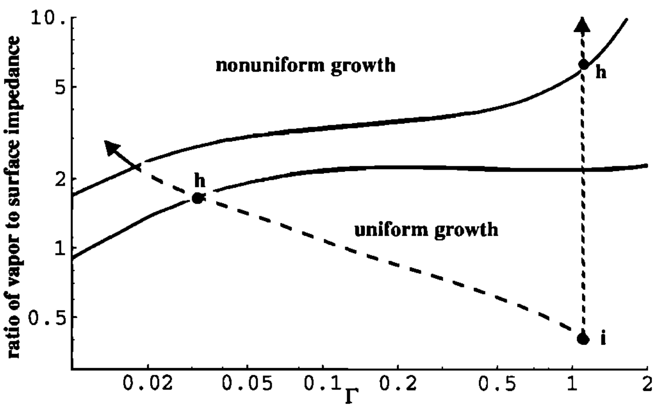

Figure 11. Regimes of uniform and nonuniform growth on the 'a' face. Top curve: boundary between uniform and nonuniform growth for a large crystal growing at dc/da = Γ that hollows at a' = 100. Bottom curve: boundary for a crystal growing at dc/da = Γ/4 that hollows at a' = 50. The arrows and symbols are discussed in the text.

on the 'a' face. Since the surface and vapor impedances are the same on both faces in this case (eqs. (25) and (29)), the basal face should hollow during growth before the prism face for isometric (Γ = 1) crystals. This is due to the fact that the centers of the basal faces are more "surrounded" by regions of uniform vapor sink than the centers of the prism faces, so that the local mixing ratio in the center of the basal faces is reduced to a greater extent, thus requiring a greater surface impedance for uniform growth. This result is in agreement with data from *Takahashi et al.* [1991].

Mason [1993] predicts that hollowing is independent of growth rate and occurs when the size of a face becomes larger than some critical value. This appears to be inconsistent with the habit diagram [see, for instance, *Mason*, 1993, Figure 1] and experimental results from *Colbeck* [1983] since these authors show hollow crystals only at large supersaturations. (Unfortunately, the crystal sizes in their diagrams were not noted.) In laboratory studies by one of us (JN), we have observed that when different prism faces grow at different rates, the faster growing (and generally, smaller area) faces hollow first, as shown in Figure 13. This is in direct contradiction to Mason's prediction but consistent with ours.

6. Discussion

The goal of this work was to derive a physically consistent but computationally useful formalism for the study of the evolution of three-dimensional ice crystals in air. In our new formalism we assume that one growth or sublimation mechanism is active over the entire crystal surface. The vapor and heat transport to and from the surface then act in series with this surface growth mechanism. The vapor mixing ratio (and thus the surface supersaturation) varies over the surface. We have assumed that ledges are generated at some point on each face, either because there are defects or dislocations or other nucleation sites there. The ledges (which contain the most likely growth sites) then spread out over the face. The rate of production of ledges at the generation point thus controls the spacing of ledges all over the face. We assume that as the ledges spread from their point of origin to points of different local supersaturation, their spreading velocity changes, and their spacing thus changes also (so that the density of growth sites changes) in such a way as to maintain a uniform rate of growth over the face. The relationship between α and σ_s is determined at the ledge source by the mechanism producing the ledges. (See, for example, eq (14).) This constraint enables us to calculate the flux at the ledge generation point on each face and thus to know the flux everywhere on the face. We assume that this description can apply to sublimation as well as to growth, but the ledge generation mechanisms and positions may be different in the two cases.

The formalism we have derived allows us to compute g/s rates and the conditions for uniform growth of finite cylindrical crystals in terms of surface parameters that must ultimately be derived from experiment.

6.1. Laboratory Observations of Ice Crystal G/S Rates

We have presented theoretical arguments showing that surface processes limit g/s rates and growth character of crystals under certain environmental conditions. Direct verification for this contention is very difficult to acquire from experimental results published in the literature, but we now examine data from laboratory and field experiments that indirectly support this conclusion. We show there are wide variations in g/s behavior from the various laboratory experiments (and we know of none performed in conditions applicable to cirrus) but that in all the experiments there is evidence that the surface impedance plays a very important role in determining the evolution of the crystals.

6.1.1. G/S rates in air. There have been three types of laboratory measurements of g/s rates in air; those in which the crystals are situated on a substrate, those in which they are suspended from/on a fiber, and those in which they are in free-fall. We now discuss each type briefly in turn.

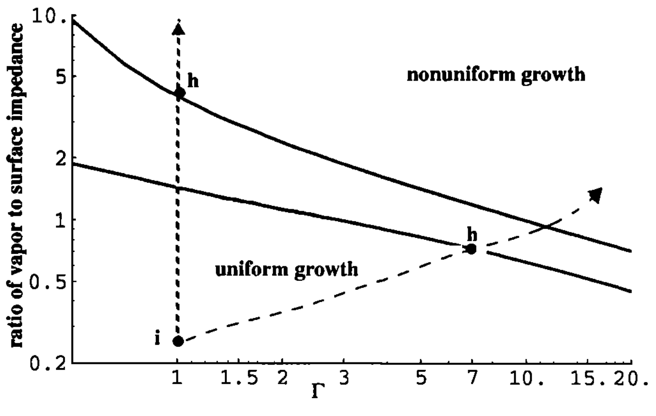

Figure 12. Regimes of uniform and nonuniform growth on the 'c' faces. Top curve: boundary between uniform and nonuniform growth for a large crystal growing at dc/da = Γ that hollows at c' = 100. Bottom curve: boundary for a crystal growing at dc/da = 4Γ that hollows at c' = 50. The arrows and circles are discussed in the text.

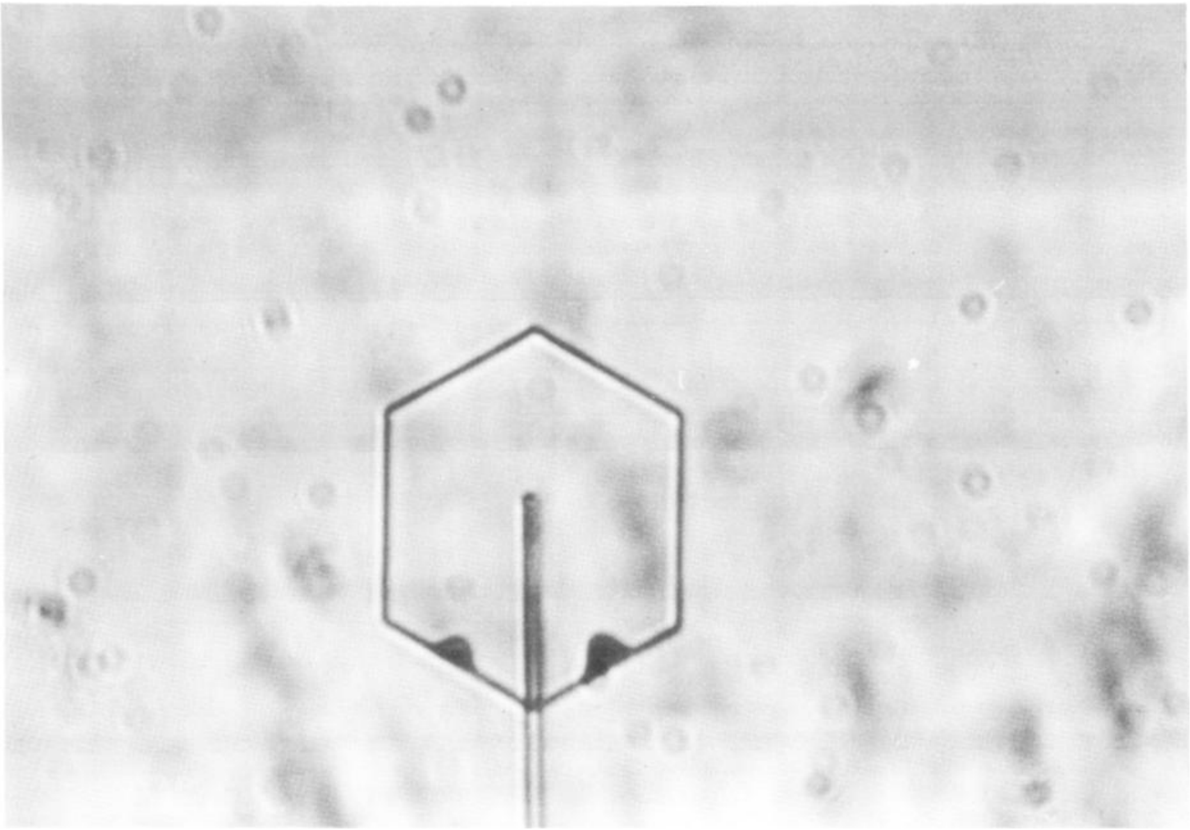

Figure 13. Platelike ice crystal grown in nearly 1 atmosphere of air. The crystal began growth at the tip of the glass capillary shown penetrating the crystal from the bottom. The 2 prism faces on the bottom grew faster (they are farther from their point of origin.) The fact that they hollowed first even though their areas are smaller than the neighboring prism faces is in direct contradiction to the prediction of *Mason* [1993].

The only experimental data on ice crystal growth rates in air at a range of supersaturations for small (<100 μm) hexagonally shaped ice crystals are those of *Shaw and Mason* [1955] (hereafter referred to as SM). Growing crystals on a metal substrate, they found that the crystal growth rates were of the form

$$\frac{da}{dt} = \frac{k_a \sigma_\infty^2}{a}, \quad \frac{dc}{dt} = \frac{k_c \sigma_\infty^2}{c}, \tag{32}$$

where $k_{a,c}$ depended only on temperature [*Shaw*, 1955]. Equation (32) also held during sublimation with $k_{a,c} \rightarrow -k_{a,c}$. (Note that shielding of one crystal, or crystal face by neighboring crystals, or interaction through the vapor, probably influenced the SM measurements because it can significantly reduce g/s rates even at relatively large crystal separations [*Labowsky*, 1976].) At very large undersaturations (depending on temperature and crystal) the sublimation rate increased dramatically and the crystals developed rounded edges. This behavior is expected since at low undersaturations, sublimation is believed to be due to the motion of ledges originating at fixed sources (crystal defects) on the interior of a face (as is the case at small supersaturations), while at larger undersaturations, the main source of ledges is expected to be from the edges. There was noticeable variation in growth rate among crystals growing under the same conditions, and the growth rate on a given crystal face was observed to change by as much as 50% without a change in the surrounding conditions. These two observations suggest that the surface impedance, which could differ for different crystals even when they are in identical environments, was larger than the vapor impedance. Also note that the dependence of dc/dt and da/dt on σ_∞^2 instead of σ_∞ is suggestive of a strong role of the surface impedance, which is highly dependent on supersaturation. (See Figure 1.)

Gonda and Koike [1982, 1983] grew ice crystals on a glass substrate in one atmosphere of air and found, like SM, that the growth rate increased faster than linearly with σ_∞. In both of these cases, at all temperatures and environmental supersaturations the observed g/s rates were less than 1/2 of the rates predicted using equation (25) with negligible surface impedance. The surface impedance was probably an important factor reducing the g/s rates.

Keller and Hallett [1982], and *Alena et al.* [1990] examined ice crystal growth on a suspended fiber and found that $da/dt \propto \sigma_\infty^n$ with $n > 1$ for supersaturations less than approximately liquid water saturation. This is consistent with the observations of both SM and those of Gonda and Koike and is an indication of a strong influence of surface impedance on growth. *Rottner and Vali* [1974] grew ice crystals on a fiber in a diffusion chamber and found that the

Table A1. List of Symbols

Symbol [dimension]	Meaning	First Appears
a,c [m]	crystal radius, 1/2 of crystal length	Figure 4
a', c'	dimensionless volume impedances	(9), (21)
'a','c'	designates the 2 types of faces	Figure 4
D_g [m^2/s]	diffusion constant of vapor in gas	(2)
$F_v \left[\frac{m\ kg(H_2O)}{s\ kg(air)}\right]$, F'_v	vapor flux, dimensionless value	(2), (22)
F_h [$W/m^2\ s$]	heat flux	(7)
h^a, h^c	dimensionless mixing ratios for fluxes to 'a', 'c' faces	(23)
l [J/molecule], l'	latent heat of sublimation, dimensionless latent heat	(8), (9)
m, M [Kg]	mass of a water molecule, crystal	(8), (27)
n^a, n^c	condensation coefficient parameter	(14)
$q_s, q_{eq} \left[\frac{kg(H_2O)}{kg(air)}\right]$	surface, equilibrium mixing ratio	(1)
T, T_s [K]	gas, crystal temperatures	(4)
$\bar{v}$ [m/s]	mean vapor molecule speed	(6)
α	condensation coefficient function	(6)
κ_g [J/K m s]	thermal conductivity of air	(7)
$\Delta q'$	shifted, dimensionless mixing ratio	(16)
Γ	aspect ratio	(21)
ρ_{air}, ρ_{ice} [Kg/m^3]	density of air, ice	(8), (13)
σ_1^a, σ_1^c	condensation coefficient parameter	(14)
σ_s, σ_∞	ambient, surface supersaturation	(6), (11)

growth rate was significantly lower than the capacitance model estimates, even at water saturation. However, in this type of experiment, shielding probably reduced the growth rates since there were many crystals along the fiber.

Colbeck [1983] investigated the growth of large ice crystals on a hair at low supersaturations. The growth rate was less than that predicted from the capacitance model, especially at lower supersaturations and lower temperatures. At a given temperature the growth rate was closer to the capacitance prediction when the supersaturation was higher, as we predict.

Takahashi et al. [1991] found that the growth rates of freely falling crystals at water saturation were within a factor of 2 of the rates predicted by the ellipsoidal capacitance model, i.e., significantly higher than those of the substrate-grown ice crystals for the same conditions. Theoretically, as pointed out earlier, we expect that the capacitance model should be a better approximation as the supersaturation increases.

6.1.2. G/S rates in pure water vapor. There have been several experiments on the growth rate of ice in a pure vapor environment [*Lamb and Scott*, 1972; *Beckmann and Lacmann*, 1982; *Sei and Gonda*, 1989]. In all of these studies, large (~100 μm) crystals were grown on a substrate, and therefore heat conduction effects reduced the growth rates considerably [*Nelson*, 1993]. It is also apparent that ice crystals grown on a substrate grow by a dislocation mechanism. Since freely growing ice crystals (i.e. without influence from another surface) appear to grow without dislocations [*McKnight and Hallett*, 1978; *Mizuno*, 1978; *Frank*, 1982], care is needed when extrapolating results inferred from substrate-based experiments to atmospheric ice crystal growth.

6.2. Observations of Ice Crystal Hollowing

While there are a number of field studies of cirrus microphysics in the literature, [e.g., *Heymsfield and Platt*, 1984; *Heymsfield*, 1977; *Sassen et al.*, 1989a; *Platt et al.*,1989; *Arnott et al.*,1994; *Ström and Heintzenberg*, 1994], instrumental limitations have precluded the collection of the dynamical and microphysical information needed to deduce g/s rates of small crystals in and near clouds. However, some information on surface parameters can be inferred from examination of crystal shapes.

Figures 11 and 12 show that according to our model in steady state growth the surface impedance must be larger than approximately 1/5th of the vapor impedance on at least one face in order for crystals to grow with flat faces. (This fraction is larger for crystals with a larger growth rate anisotropy.) In some cirrus clouds, uniformly growing crystals are relatively common [*Heymsfield and Platt*, 1984; *Miloshevich and Heymsfield*, 1992]. When both solid and hollow columns are observed in cirrus, the conditions may be such that the crystals are growing near the border between uniform and nonuniform growth and therefore the surface impedance is roughly equal to the magnitude of the vapor impedance. Note, however, that it is also possible that the hollowing occurred during the early phase of cloud formation when the supersaturation was higher due to either the existence of supercooled drops or to a lower crystal concentration. Also, it is difficult to distinguish between hollow crystals and crystals with completely enclosed voids when the crystals are small.

Gonda and Koike [1982, 1983] observed ice crystals beginning to hollow at small sizes, but at larger sizes, the growth became uniform again. For these crystals the growth rates were much less than those predicted on the basis of the capacitance model, suggesting that the surface impedance was twice to 9 times the magnitude of the vapor impedance. The resulting crystals had flat faces but voids in their interior. We have made similar observations in our laboratory. These features are not uncommon in ice crystals grown in the atmosphere.

Table B1. Values of $h^a(\Gamma)$, $h^c(\Gamma)$

Γ	$h^a(\Gamma)$	$h^c(\Gamma)$
0.01	0.0233	62.0
0.05	0.0900	11.7
0.1	0.155	5.62
0.2	0.258	2.65
0.25	0.300	2.07
0.27	0.316	1.90
0.5	0.469	0.959
0.82	0.622	0.554
1	0.690	0.445
2	0.963	0.208
2.5	1.06	0.164
2.7	1.09	0.151
5	1.38	0.0781
10	1.70	0.0374
20	2.05	0.0184

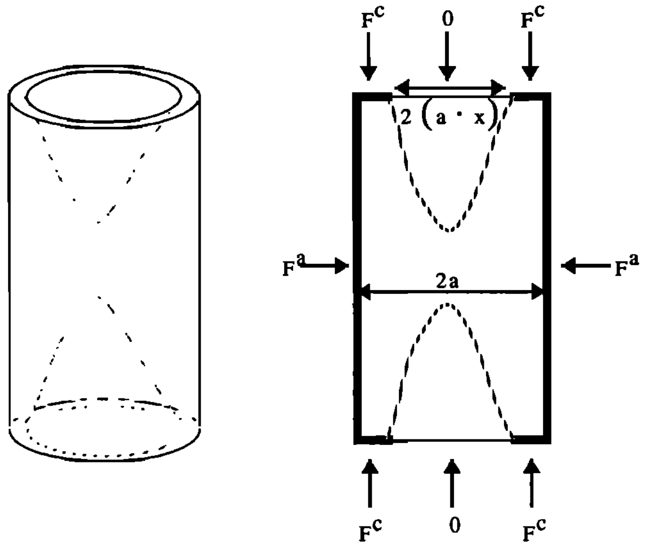

Figure 14. A hollow column (left) has uniform growth on the 'a' face and only a small region of the 'c' face (right). We will assume that the flux to the region within a · x of the 'c' face center is zero.

In the last two sections we have examined three types of observations of ice crystals in order to estimate the magnitude of the surface impedance during ice crystal growth and sublimation. Most are consistent with the hypothesis that surface impedance is comparable to vapor impedance under the conditions examined except at high supersaturations and large crystal sizes. Although large experimental uncertainties presently prevent a truly quantitative formulation of vapor g/s rates of small ice crystals, the formalism we have presented here presents the theoretical basis for examination of the evolution of three-dimensional crystals in air.

7. Applications

Our new model is quite general. For its application we depend on knowledge of the relationship between surface impedance and local supersaturation. The form of this relationship can be derived from a model of the surface (for example, see equation (14)), but any such relationship contains parameters that must ultimately be derived from experiment. We have shown that surface processes play important roles in limiting the g/s rates and aspect ratios of atmospheric ice crystals under conditions expected in and near fully glaciated clouds. Crystals in this part of the atmosphere play important roles in radiative and chemical processes, and these roles are determined largely by the shape and sizes of the crystals as well as the surface structure. There is laboratory evidence that small concentrations of gaseous impurities alter the crystal growth shape [*Anderson et al.*,1969; *Hallett and Mason*, 1958; *Nakaya et al.*,1958; *Neustaedter and Gallily*, 1987; *Odencrantz*, 1968; *Schaefer*, 1949]. The uniform flux model (as opposed to the capacitance model) readily lends itself to exploration of these impurity-induced modifications of surface impedance [*Nelson*, 1994]. It has been suggested that gas phase impurities hinder sublimation in the upper troposphere [*Peter et al.*,1994]. Thus further theoretical and experimental exploration of crystal evolution under these conditions is needed for further progress on these important topics and directed field studies would aid in investigating the applicability of both the capacitance and the uniform flux models to the atmosphere. Laboratory experiments in progress lend support to the uniform flux model presented here and our results will be described in future publications.

Appendix A: Symbols

Appendix B: Mixing Ratio Functions $h^{c,a}$

The method used here to solve for $\Delta q'$ is to split up the region surrounding the crystal into subregions chosen in such a way as to permit use of the method of separation of variables. Along the common boundaries between 2 regions the vapor mixing ratio and gradient of the vapor mixing ratio are set equal to each other. The functions $h^{c,a}$ which appear in equation (23) are defined in terms of matrix operations on the eigenvectors in each region and will not be given here except for certain positions on the crystal surface. It can be shown that a crystal with n independent faces will have n terms on the RHS of equation (23), one for each F'. A complete description of this method is found in the work of *Nelson* 1994. Because of the large sizes of the matrices involved, $h^{c,a}$ were calculated explicitly at discrete values of Γ only. Values of the functions $h^a(\Gamma)$, $h^c(\Gamma)$ are given below. Approximate analytic fits are

$$h^c(\Gamma) \approx \frac{1.15}{\pi\Gamma} + \frac{0.85}{2\pi\Gamma} \cdot (1 - \tanh[0.947 \cdot \log_{10}[\Gamma] + 0.477])$$

$$h^a(\Gamma) \approx 0.663 \cdot \log_{10}[1 + 1.85 \cdot \Gamma^{0.894}]^{0.937} \quad . \quad \text{(B1)}$$

Appendix C: Growth of Hollow Crystals

The technique developed above for solid crystals can also be used to describe the growth of very hollow crystals in an approximate manner. Assume that on the 'c' faces of a hollow column, growth occurs only along a small ring of width $a(1-x)$ (Figure 14). We take advantage of the linearity of the problem to solve for the growth rate using superposition of solutions. If $x \approx 1$, the resulting mixing ratio Δq_h is nearly equal to the value obtained by subtracting the mixing ratio Δq_0 (finite cylinder with uniform flux F^c on the 'c' face and no flux on the 'a' face, aspect ratio Γ/x) from the mixing ratio Δq_1 of the solid cylinder with uniform fluxes F^c, F^a, aspect ratio Γ. That is, eq (23) is replaced by

$$\Delta q_h \approx -F'^c(h^c(\Gamma) - h^c(\Gamma/x)) - F'^a h^a(\Gamma) . \quad \text{(C1)}$$

Thus the uniform flux model also applies to very hollow crystals with the substitution $h^c(\Gamma) \rightarrow h^c_h \equiv h^c(\Gamma) - h^c(\Gamma/x)$. Since $h^c(\Gamma) \approx g/\Gamma$ (see equation (B1)) where g is nearly independent of Γ, then $h^c_h \approx h^c(1-x) \ll h^c$.

If the ledge sources are on the edge for both faces before hollowing, then this change in mixing ratio will have little effect on dc/da after hollowing. However, crystal hollowing can change the evolution of crystal aspect ratios. Consider a crystal on which α^c/α^a is large initially. The surface mixing ratio (assuming no hollowing) then becomes largest in the center of the 'a' face (see Figure 9). Since the 'a' face now has a larger mixing ratio, it can grow faster and thus reduce the magnitude of the growth rate anisotropy ($dc/da < \alpha^c/\alpha^a$). Hollowing changes this picture by increasing the magnitude of the mixing ratio at the edge. This allows $dc/da = \alpha^c/\alpha^a$ to remain large, resulting in a greater aspect ratio for the hollow crystal than for the solid one. This argument applies equally well to hollowing on the 'a' face. Thus hollowing is an important process for the formation of crystals with large aspect ratios.

Acknowledgments. J. Nelson was supported throughout this work by a NASA Global Change Fellowship and a DOE Distinguished Global Change Postdoctoral Fellowship. MBB was partially supported by NSF grant ATM 92-23563. NCAR is supported by the National Science Foundation. We gratefully acknowledge very helpful comments and suggestions by M. Baker, J. Y. Harrington, and from two anonymous reviewers.

References

Alena, T., J. Hallett, and C. P. R. Saunders, On the face-skeletal transition of snow crystals: Experiments in high and low gravity, *J. Cryst. Growth, 104,* 539-555, 1990.

Anderson, B.J., J.D. Sutkoff, and J. Hallett, Influence of methyl 2-cyanoacrylate monomer on the habit of ice crystals grown from the vapor, *J. Atmos. Sci., 26,* 673-674, 1969.

Arnott, W. P., Y. Y. Dong, and J. Hallett, Role of small ice crystals in radiative properties of cirrus: A case study, FIRE II, November 22, 1991, *J. Geophys. Res., 99,* 1371-1381, 1994.

Auer, A.H., Jr., and D.L. Veal, The dimension of ice crystals in natural clouds, *J. Atmos. Sci., 27,* 919-926, 1970.

Beckmann, W., and R. Lacmann, Interface kinetics of the growth and evaporation of ice single crystals from the vapour phase II, Measurements in a pure water vapour environment, *J. Cryst. Growth, 58,* 433-442, 1982.

Burton, W. K., N. Cabrera, and F.C. Frank, The growth of crystals and the equilibrium structure of their surface, *Proc. R. Soc. Lond. A, 243,* 299-358, 1951.

Chen, J. P., and D. Lamb, The theoretical basis for the parameterization of ice crystal habits: Growth by vapor deposition, *J. Atmos. Sci., 51,* 1206-1221, 1994.

Colbeck, S. C., Ice crystal morphology and growth rates at low supersaturations and high temperatures, *J. Appl. Phys., 54,* 2677-2682, 1983.

Frank, F.C., Snow crystals, *Contemp. Phys., 23,* 3-22, 1982.

Fukuta, N., and L. A. Walter, Kinetics of hydrometeor growth from a vapor-spherical model, *J. Atmos. Sci., 27,* 1160-1172, 1970.

Gonda, T., The influence of the diffusion of vapor and heat on the morphology of ice crystals grown from the vapor, *J. Cryst. Growth, 49,* 173-181, 1980.

Gonda, T., and T. Koike, Growth rates and growth forms of ice crystals grown from the vapor phase, *J. Cryst. Growth, 56,* 259-269, 1982.

Gonda, T., and T. Koike, Growth mechanisms of single ice crystals growing at a low temperature and their morphological stability, *J. Cryst. Growth, 65*, 36-48, 1983.

Goodman, F. O., Thermal accommodation coefficients, *J. Phys. Chem., 84*, 1431-1445, 1980.

Hallett, J., and B. J. Mason, Influence of organic vapours on the crystal habit of ice, *Nature, 181*, 467-468, 1958.

Heymsfield, A.J., Precipitation development in stratiform ice clouds: A microphysical and dynamical study, *J. Atmos. Sci., 34*, 367-381, 1977.

Heymsfield, A. J., and L. M. Miloshevich, Homogeneous ice nucleation and supercooled liquid water in orographic wave clouds, *J. Atmos. Sci., 50*, 2335-2353, 1993.

Heymsfield, A.J., and C.M.R. Platt, A parameterization of the particle size spectrum of ice clouds in terms of the ambient temperature and the ice water content, *J. Atmos. Sci., 41*, 846 -855, 1984.

Keller, V. W., and J. Hallett, Influence of air velocity on the habit of ice crystal growth from the vapor, *J. Cryst. Growth, 60*, 91-106, 1982.

Kinne, S., and K. N. Liou, The effects of the nonsphericity and size distribution of ice crystals on the radiative properties of clouds, *Atmos. Res., 24*, 273-284, 1989.

Kobayashi, T., and T. Kuroda, Snow crystals, in *Morphology of Crystals*, edited by I. Sunagawa, pp. 645-743, Terrapub, Tokyo, 1987.

Kuroda, T., Rate determining processes of growth of ice crystals from the vapour phase, I, Theoretical consideration, *J. Meteorol. Soc. Jpn., 62*, 552-561, 1984.

Labowsky, M., The effects of nearest neighbor interactions on the evaporation rate of cloud particles, *Chem. Eng. Sci., 31*, 803-813, 1976.

Lamb, D., and W. D. Scott, Linear growth rates of ice crystals grown from the vapor phase, *J. Cryst. Growth, 12*, 21-31, 1972.

Mackenzie, A. R., and P. H. Haynes, The influence of surface kinetics on the growth of stratospheric ice crystals, *J. Geophys. Res., 97*, 8057-8064, 1992.

Mason, B. J., Growth habits and growth rates of snow crystals, *Proc. R. Soc. Lond. A, 441*, 3-16, 1993.

Mason, B. J., G. W. Bryant, and A. P. van den Heuvel, The growth habits and surface structure of ice crystals, *Philos. Mag., 8*, 505 -526, 1963.

McKnight, C. V., and J. Hallett, X-ray topographic studies of dislocations in vapor-grown ice crystals, *J. Glaciol., 21*, 397-407,1978.

Miloshevich, L., and A. Heymsfield, Microphysical measurements in cirrus clouds from ice crystal replicator sondes launched during fire II, paper presented at 11th International Conference on Clouds and Precipitation, AMS., Montreal, 525-528, 1992.

Ming, N-B., K. Tsukamoto, I. Sunagawa, and A.A. Chernov, Stacking faults as self-perpetuating step sources, *J. Cryst. Growth, 91*, 11-19, 1988.

Mizuno, Y., Studies of crystal imperfections in ice with reference to the growth process by the use of X-ray diffraction topography and divergent laue method, *J. Glaciol., 21*, 409-418, 1978.

Morse, P., and H. Feshbach, *Methods of Theoretical Physics*, II, Chap. 10, McGraw-Hill, New York, 1953.

Nakaya, U., M. Hanajima, and J. Muguruma, Physical investigations on the growth of snow crystals, *J. Fac. Sci., Hokkaido University, Jpn, Ser. II, 5(3)*, 88-132, 1958.

Nelson, J.T., Heat conduction problems in crystal growth from the vapor, *J. Cryst. Growth, 132*, 538-550, 1993.

Nelson, J.T., A theoretical study of ice crystal growth in the atmosphere, Ph. D. dissertation, Univ. Washington, Seattle, 1994.

Neustaedter, J., and I. Gallily, Some aspects of ice crystal growth from the vapour phase; Apparatus and growth kinetics in the presence of organic gases and with various nucleants, *J. Cryst. Growth, 85*, 422-432, 1987.

Odencrantz, F. K., Modification of habit and charge of ice crystals by vapor contamination, *J. Atmos. Sci., 25*, 337-338, 1968.

Peter, T., R. Muller, P. J. Crutzen, and T. Deshler, The lifetime of leewave-induced ice particles in the arctic stratosphere: II, Stabilization due to NAT-coating, *Geophys. Res. Lett., 21*, 1331-1334, 1994.

Platt, C. M. R., J. D. Spinhirne, and W. D. Hart, Optical and microphysical properties of a cold cirrus cloud: Evidence for regions of small ice particles, *J. Geophys. Res., 94*, 11,151-11,164, 1989.

Ramaswamy, V., and A. Detwiler, Interdependence of radiation and microphysics in cirrus clouds, *J. Atmos. Sci., 43*, 2289-2301, 1986.

Rottner, D., and G. Vali, Snow crystal habit at small excesses of vapor density over ice saturation, *J. Atmos. Sci., 31*, 560-569, 1974.

Sassen, K., M.K. Griffin, and G.C. Dodd, Optical scattering and microphysical properties of subvisual cirrus clouds, and climatic implications, *J. Appl. Meteorol., 28*, 91-98, 1989a.

Sassen, K., D. O'C. Starr, and T. Uttal, Mesoscale and microscale structure of cirrus clouds: Three case studies, *J. Atmos. Sci., 46*, 371-396, 1989b.

Schaefer, V.J., The formation of ice crystals in the laboratory and the atmosphere, *Chem. Rev., 44*, 291-320, 1949.

Seeger, A., Diffusion problems associated with the growth of crystals from dilute solution, *Philos. Mag., 44*, 1-13, 1953.

Sei, T., and T. Gonda, The growth mechanism and the habit change of ice crystals growing from the vapor phase, *J. Cryst. Growth, 94*, 697-706, 1989.

Shaw, D., The growth of ice crystals, Ph.D. dissertation, Univ. of London, 1955.

Shaw, D., and B. J. Mason, The growth of ice crystals from the vapour, *Philos. Mag., 46*, 249-262, 1955.

Ström, J., and J. Heintzenberg, Water vapor, condensed water, and crystal concentration in orographically influenced cirrus clouds, *J. Atmos. Sci., 51*, 2368-2383, 1994.

Surek, T., Evaporation of crystals by a ledge mechanism, Ph.D. dissertation, Stanford University, Palo Alto, Calif., 1972.

Takahashi, T., T. Endoh, G. Wakahama, and N. Fukuta, Vapor diffusional growth of free-falling snow crystals between -3 and -23C, *J. Meteorol. Soc. Jpn., 69*, 15-32, 1991.

van der Eerden, J. P., Crystal growth mechanisms, in *Handbook of Crystal Growth* 1, *Fundamentals*, Part A; *Thermodynamics and Kinetics*, Edited by D. T. J. Hurle, North-Holland, New York, 1993.

Wallace, J. M., and P. V. Hobbs, *Atmospheric Science; an Introductory Survey*, Academic, San Diego, Calif., 1977.

M. B. Baker, Geophysics Program, University of Washington, Box 351650, Seattle, WA 98195-1650.

J. T. Nelson (corresponding author), NCAR, P. O. Box 3000, Boulder, CO 80307-3000.

(Received December 28, 1994; revised August 22, 1995; accepted September 14, 1995.)